WATER RESOURCES RESEARCH, VOL. 27, NO. 10, PAGES 2695–2705, OCTOBER 1991

The Las Cruces Trench Site: Characterization, Experimental Results, and One-Dimensional Flow Predictions

P. J. WIERENGA

Department of Soil and Water Science, University of Arizona, Tucson

R. G. HILLS

Mechanical Engineering Department, New Mexico State University, Las Cruces

D. B. HUDSON

Department of Soil and Water Science, University of Arizona, Tucson

A comprehensive field trench study was conducted in a semiarid area of southern New Mexico to provide data to test deterministic and stochastic models of vadose zone flow and transport. A 4 m by 9 m area was irrigated with water containing a tracer using a carefully controlled drip irrigation system. The area was heavily instrumented with tensiometers and neutron probe access tubes to monitor water movement and with suction tubes to monitor solute transport. Approximately 600 disturbed and 600 core samples of soil were taken to support deterministic and stochastic characterization of the soil water hydraulic parameters. The core sample–based saturated hydraulic conductivities ranged from 1.4 to 6731 cm/d with a mean of 533 cm/d and a standard deviation of 647 cm/d, indicating significant spatial variability. However, visual observation of the wetting front on the trench wall shows no indication of preferential flow or water flow through visible root channels and cracks. The tensiometer readings and the neutron probe measurements also suggest that the wetting front moves in a fairly homogeneous fashion despite the significant spatial variability of the saturated hydraulic conductivity. In addition to the description of the experiment and the presentation of the experimental results, predictions of simple one-dimensional uniform and layered soil deterministic models for infiltration are presented and compared to field observations. These models are presented here to provide a base case against which more sophisticated deterministic and stochastic models can be compared in the future. The results indicate that the simple models give adequate predictions of the overall movement of the wetting front through the soil during infiltration. However, the models give poor predictions of point values for water content due to the spatial variability of the soil. Comparisons between the one-dimensional infiltration model predictions and field observations show that the use of the layered soil model rather than the uniform soil model does not consistently improve the accuracy of the predictions for this particular field application. This result illustrates that increasing the spatial resolution of the deterministic characterization of the site in the vertical direction does not always improve the model predictions. Uncertainties due to horizontal spatial variability and due to other difficulties associated with experimental characterization appear to be more significant.

INTRODUCTION

Prediction of water flow and chemical transport from disposal areas generally requires the use of computer models. There are many deterministic numerical models available for use in homogeneous, two-dimensional, saturated or unsaturated systems. Due to the lack of sufficient field data, the validity of these models as applied to dry soils on the field scale has not been adequately tested. Field studies in soil science and hydrology conducted during the past decade have demonstrated extensive variability in saturated and unsaturated hydraulic conductivities and water retention properties [*Biggar and Nielsen*, 1976; *Warrick and Nielsen*, 1980; *Peck*, 1983; *Webster and de la Cuanalo*, 1975]. Such developments have cast doubt on the validity of deterministic models when applied on the field scale. This has led to the development of stochastic models for the prediction of water flow and chemical transport through soils and groundwater [*Russo and Bresler*, 1981; *Dagan and Bresler*, 1979; *Gelhar and Axness*, 1983]. However, before such models will find widespread use for prediction purposes, the advantage of stochastic models over simpler deterministic models must first be validated using field data. This poses a problem. Stochastic models require statistical information on the relevant soil properties such as the mean, variance, and correlation length of hydraulic properties. Unfortunately, few data sets are available which include information on the statistical distribution and spatial dependence of the important hydraulic properties.

The purpose of this field study is to develop a data base for testing deterministic flow and transport models as well as the stochastic models developed by Gelhar and associates [*Montaglou and Gelhar*, 1985; *Yeh et al.*, 1985*a*, *b*, *c*]. A detailed field experiment was designed in cooperation with Lynn Gelhar, Massachusetts Institute of Technology, and Glendon Gee, Battelle Pacific Northwest Laboratories, to study the movement of water containing a chemical tracer through an initially dry, spatially variable soil. Great efforts were made to characterize the soil at the experimental site in

Paper number 91WR01537.
0043-1397/91/91WR-01537$05.00.

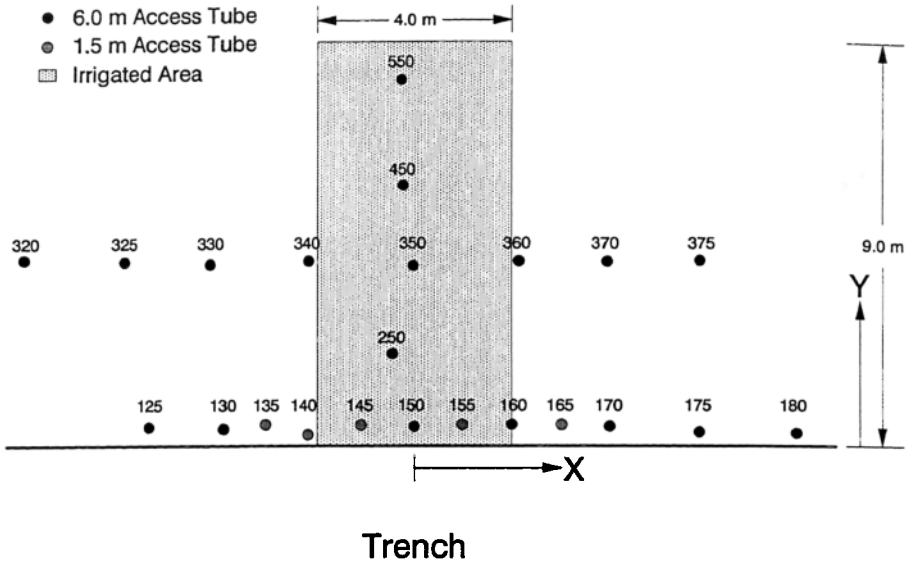

Fig. 1. Plan view of the trench face, the irrigated area, and the neutron access tubes.

sufficient detail so that deterministic and stochastic models for the hydraulic properties could be estimated.

The purpose of this paper is to provide an introduction to the characterization and to describe a dynamic experiment, to outline the experimental methods used to characterize and monitor the site, and to present some of the experimental results on water flow obtained during the early phases of the dynamic experiment.

Finally, we used some of the hydraulic property models generated during site characterization in conjunction with simple one-dimensional deterministic numerical models for Richards' equation to predict infiltration at the site. These simple deterministic models provide base cases against which more sophisticated deterministic and stochastic models can be tested in the future.

METHODS, MATERIALS AND THEORY

Site Description and Characterization

The experimental site is located on the New Mexico State University college ranch, about 40 km northeast of Las Cruces, New Mexico. The site is on a basin slope of Mount Summerford at the north end of the Dona Ana Mountains. The Dona Ana Mountains form a domal uplift complex of younger rhyolitic and the older andesitic volcanics intruded by monzonite. Climate in the region is characterized by an abundance of sunshine, low relative humidity and an average class A pan evaporation of 239 cm per year. Average annual precipitation is 23 cm [*Wierenga et al.*, 1987]. A 26.4 m long by 4.8 m wide by 6.0 m deep trench was constructed in the undisturbed soil to provide horizontal access to an irrigated plot and to provide soil samples. A 4 m by 9 m area was selected on the south side of the trench (see Figure 1) for controlled application of water containing a tracer.

After excavation of the trench, nine soil layers were identified based on the observed morphological horizons on the west wall of the trench and on the hydraulic properties of each layer. This was done by grouping the morphological soil horizons with similar hydrological properties. These nine layers are shown as different shades in Figure 2.

The uppermost layer (0.00–0.15 m depth) shows some organic matter accumulation and some evidence of clay eluviation. There are many roots in this layer. The soil is not effervescent and its structure is massive. The soils of the deeper layers range from slightly to strongly effervescent and possess a subangular blocky structure. The average bulk density for the nine layers ranges from 1.66 to 1.74 g/cm^3. Average $CaCO_3$ content ranges from 1.4% in the top layer to 22.6% in the eighth layer. The average coarse fraction ranges from 19.5% in layer 3 to 34.6% in layer 9. The results of the particle size analysis of the 50 soil samples taken from each layer indicate that the soils are sands, sandy loams, loamy sands, and sandy clay loams. Layers 2, 3, 4, 6, 8, and 9 show

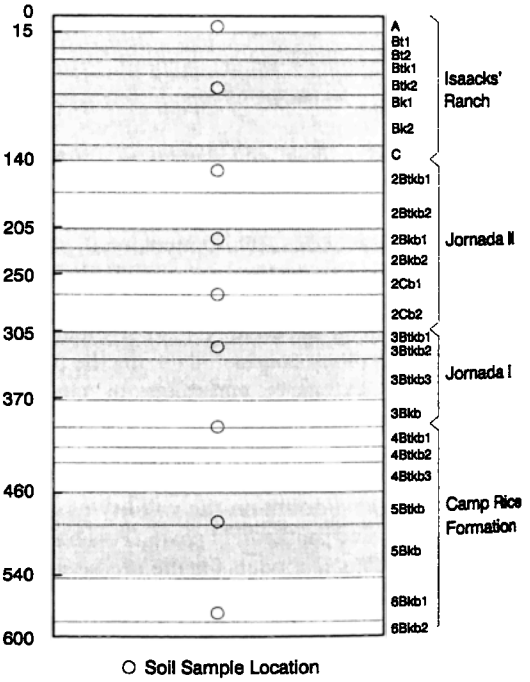

Fig. 2. Morphological horizons at the Las Cruces trench site.

evidence of carbonate accumulation. There are various buried arroyos visible along the trench walls. The soil in these buried arroyos has no structure and the texture is gravelly sandy loam. A more detailed discussion on the soil morphology at the Las Cruces site is presented by *Wierenga et al.* [1989].

Fifty undisturbed core samples and 50 disturbed soil samples were taken along the north wall of the trench at 0.5 m intervals (in the horizontal direction) from each of the nine soil layers. The sampling depths for the center of the soil core samples were 0.11, 0.71, 1.51, 2.16, 2.70, 3.20, 3.98, 4.89, and 5.79 m. The undisturbed soil core samples were collected in 7.6-cm-ID by 7.6-cm-long aluminum rings. Each disturbed soil sample consisted of approximately 425 g of loose soil. To provide data to determine the vertical correlation length, cores and disturbed soil samples were also taken at approximately 13 cm depth intervals to a depth of 6.1 m in the vertical direction at three locations along the length of the trench. Altogether, a total of 594 soil cores and 594 disturbed soil samples were taken to the laboratory for the estimation of their bulk density, saturated hydraulic conductivity and the soil water retention curve.

The saturated hydraulic conductivity of the soil was determined in situ with the Guelph permeameter method [*Reynolds and Elrick*, 1985]. Ten-centimeter-diameter by 15-cm-deep holes were drilled in the undisturbed soil 30 cm to the side of each location where core samples were taken (50 per soil layer spaced 0.5 m apart for each of the nine soil layers) along the north trench wall. Using the Guelph permeameter, a constant water level was maintained in each hole and the rate of flow into each hole measured. The results from these measurements are presented by *Wierenga et al.* [1988, 1989] and discussed by *Jacobson* [1988, 1990].

The saturated hydraulic conductivity of each core was also measured by applying a constant head differential across the cores and measuring the outflow using the method of *Elrick et al.* [1980]. The wet range of the soil water retention curves was determined by placing the saturated cores from each location into pressure boxes, subjecting them to differential pressures of 10, 20, 40, 80, 120, 200, and 300 cm H_2O, and measuring the total outflow at each differential pressure. Once outflow ceased at 300 cm H_2O pressure, the cores were oven dried at 105°C for at least 7 days and the bulk density and water contents determined. The disturbed soil samples from each location were sieved and air-dried and used with a standard pressure plate apparatus (Soil Moisture Equipment Co., Santa Barbara, California) to determine soil water retention data in the 1–15 bar (dry) range. The NLIN procedure of SAS [*SAS Institute*, 1985] was used to find least squares estimates of the parameters α and n in van Genuchten's water retention model for each core location. This model for water retention is given by [*van Genuchten*, 1980]

$$S_e = \frac{\theta - \theta_r}{\theta_s - \theta_r} = \frac{1}{[1 + (\alpha h)^n]^m} \tag{1}$$

$$m = 1 - \frac{1}{n} \tag{2}$$

where θ, θ_r, and θ_s are the volumetric water content, residual water content, and saturated water content, respectively, α and n are the parameters to be estimated, and h is tension. The value of θ_r was set to the measured 15-bar water content value and θ_s was set to the gravimetrically measured value for each sample location. Given estimates of the parameters in (1) and laboratory estimates of the saturated conductivity, K_s, at each location, *Mualem*'s [1976] model, as simplified by *van Genuchten* [1980], can be used to predict the unsaturated hydraulic conductivity as a function of water content for each location:

$$K = K_s S_e^{1/2}[1 - (1 - S_e^{1/m})^m]^2 \tag{3}$$

In addition to estimating the hydraulic parameters that appear in (1) and (3) for each core sample, estimates for the hydraulic parameters were obtained for a uniform soil model and for a layered soil model. The layers in the layered soil model correspond to the nine soil layers identified at the site. The saturated hydraulic conductivity for each soil layer was estimated by taking the geometric mean of the 50 laboratory-measured saturated hydraulic conductivities obtained from each soil layer. Likewise, the water retention data from all 50 samples from a given layer were used to estimate α, n, θ_r, and θ_s for a single water retention curve for that layer. For the uniform soil model, the geometric mean of 450 laboratory measured saturated hydraulic conductivities (nine layers with 50 per layer) was used to estimate a uniform soil saturated hydraulic conductivity value. Likewise, the water retention data for all 450 sample locations were simultaneously used to estimate single values for each of the parameters α, n, θ_r, and θ_s in a least squares sense. This resulted in a single water retention curve (i.e., uniform soil model) for the entire site.

Monitoring Water Flow and Solute Transport

Soil samples were collected on May 2 and 3, 1988 during the installation of seven neutron probe access tubes into undisturbed dry soil on the north side of the trench. The seven tubes were approximately 1 m apart and along a transect perpendicular to the north trench wall. Soil samples were taken from nine depths for each neutron probe access tube location. The samples were taken at 0.75 m depth intervals from 0.60 m to 6.60 m. Field tensions were obtained from these soil samples using a Decagon thermocouple psychrometer (Decagon Devices Inc., Pullman, Washington).

A total of 18 neutron access tubes were installed, down to 6.1 m, on the area adjacent to the south wall of the trench to monitor water content. Five additional neutron access tubes were installed down to 1.5 m. The neutron probe access tubes were installed before excavation of the trench. The positions of the access tubes with respect to the trench and the irrigated area are presented in Figure 1. The neutron probe was calibrated at the experimental site by gravimetric sampling [*Wierenga et al.*, 1988]. Neutron probe readings were initially taken once a day, but less frequently outside the wetted area and during the redistribution phase.

Tensiometers were installed through the trench face such that the porous cup of each tensiometer was inserted 50 cm horizontally (within 10° of horizontal) into the formation. The locations of the tensiometers are shown in Figure 3. Pressures were measured through a septum stopper at the exposed end of each tensiometer. The ends of the tensiometers extended approximately 15 cm into the trench. The tension in each tensiometer was measured daily with a

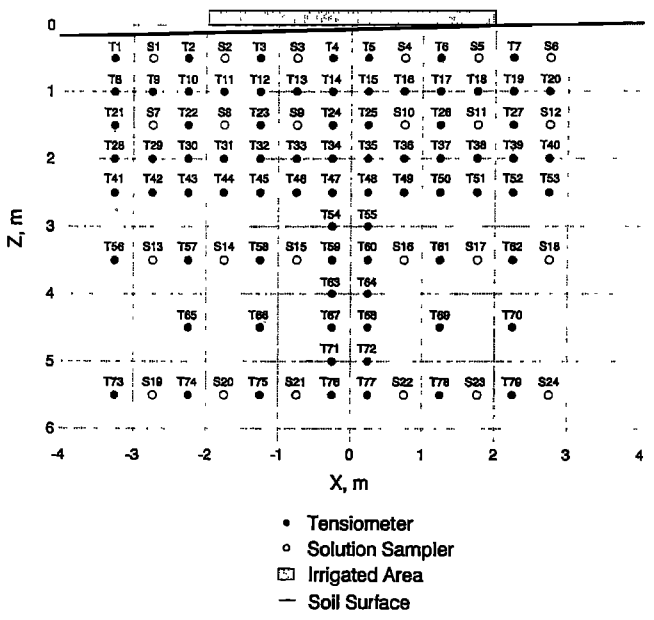

Fig. 3. Location of tensiometers and solute samplers in trench wall.

hand-held pressure transducer (Soil Measurement Systems, Tucson, Arizona) after the wetting front had reached the tensiometer. Earlier readings would be unreliable due to the very dry initial conditions and the associated high tensions.

The advance of the wetting front was determined from the neutron probe data and from the tensiometer data and was monitored on the trench face by visual observation. A 0.5 × 0.5 m grid, consisting of tight strings, was placed over the trench face so that the position of the wetting front could be sketched on graph paper.

Soil solution samplers were also installed in a grid pattern through the trench wall in the same manner as the tensiometers (see Figure 3). Once the water front had reached the samplers, a constant vacuum of approximately 200 mbar was applied to the samplers to collect daily soil solution samples.

Water Application

Water from a nearby irrigation well was applied to the 4 m by 9 m area through a closely spaced grid (approximately 0.30 m by 0.15 m) of drip emitters. Sixty irrigation lines, each containing 13 emitters, were connected to two separate header pipes, which in turn were connected to the water supply system [*Wierenga et al.*, 1988]. Water was applied four times a day for 17 min per application period, resulting in an average surface flux of 1.82 cm/day during the 86 days of the experiment. Visual inspection of the drip irrigation system during water application indicates that surface ponding was not present. The irrigated area and surrounding area were covered by a pond liner to inhibit evaporation from the surface and to prevent infiltration of rain water.

Water application to the 4 m by 9 m area was started on May 27, 1987, at a uniform rate. It was stopped on August 21 (86th day after the start of the irrigation). Tritium was added to the water during the first 10 days of water application. The concentration of applied tritium was 0.01 μCi/mL. A total of 62.6 mCi of tritium in 6260 L of water was applied to the experimental area.

Modeling One-Dimensional Deterministic Infiltration

To help evaluate the completeness of the data set for deterministic modeling applications, we performed a few simple one-dimensional numerical simulations of infiltration into the soil at the Las Cruces trench site. More sophisticated deterministic and stochastic models are currently being tested by us and other authors and the results will be reported in the future. Richards' equation for one-dimensional water flow in a saturated-unsaturated soil is given by

$$\frac{\partial \theta}{\partial t} + \frac{\partial}{\partial z}\left(K + K\frac{\partial h}{\partial z}\right) = 0 \tag{4}$$

where θ is the volumetric water content, K is the hydraulic conductivity, h is tension, t is time, and z is the vertical position measured downward. Writing (4) in terms of water content gives

$$\frac{\partial \theta}{\partial t} + \frac{\partial}{\partial z}\left(K - D\frac{\partial \theta}{\partial z}\right) = 0 \tag{5}$$

where D is defined by

$$D \equiv -\frac{K}{\partial \theta / \partial h} \tag{6}$$

While (5) is not valid across a layer-to-layer interface, it can be applied within each layer of a layered soil. The use of (5) for a layered system requires that the discontinuities in θ across an interface be properly accounted for. *Hills et al.* [1989*a*, *b*] presented a one-dimensional water content–based finite difference algorithm to solve (5) that accounts for this discontinuity. The contact discontinuities in water content across an interface are modeled by requiring that the pressure head and the water flux be continuous across the interface. Despite the increased overhead required to ensure continuity, they found the water content–based algorithm to be much more CPU efficient than comparable head-based algorithms when modeling infiltration into layered soils with very dry initial conditions (≈ 50 bars). This algorithm is used here.

The initial and boundary conditions on $\theta(z, t)$ are modeled by:

$$\theta(z, 0) = \theta_{\text{init}}(z) = \theta(h_{\text{init}}(z)) \tag{7a}$$

$$\left(K - D\frac{\partial \theta}{\partial z}\right)\bigg|_{z=0} = 1.82 \text{ cm/d} \tag{7b}$$

$$\theta(b, t) = \theta_{\text{init}}(b) \tag{7c}$$

where b is sufficiently large (or the simulation time sufficiently small) so that the wetting front does not affect water content at $z = b$. We use $b = 5.74$ m and restrict the simulations to 35 days. The initial water content $\theta_{\text{init}}(z)$ is determined from the soil retention model (uniform or layered) using measured values for the initial tensions. These values were obtained by averaging the initial tensions observed in soil samples taken during the installation of the seven neutron probe access tubes on the north side of the trench (see earlier discussion).

DISCUSSION OF RESULTS

Characterization of Hydraulic Properties

Figure 4 shows the spatial variation of K_s as estimated in the laboratory by measuring outflow at a constant head and as estimated in the field using the Guelph permeameter method. CA-DISSPLA [*Computer Associates*, 1988] was used to produce contours from values at 450 different spatial locations. Note that the spatial distributions of the laboratory-based K_s and the in situ–based K_s data have significant differences. The figure shows qualitative agreement in the locations of the large values of K_s (i.e., at $x = -6$ m, -1 m, and 5 m). Quantitatively, however, the in situ K_s at these locations are significantly larger than the corresponding laboratory-based values. Overall, the in situ–based values show a larger range than do the laboratory-based values. The greater range for the field values of saturated hydraulic conductivity may be due to the larger effect that the horizontal component of saturated conductivity has on the in situ measurements or simply due to increased uncertainties associated with the in situ measurement technique. In either case, these results illustrate the difficulty of obtaining agreement between laboratory- and in situ–based hydraulic property measurements. The spatial variability of the van Genuchten parameters θ_s, θ_r, n, and α is discussed by *Hills et al.* [1991].

Stochastic modeling of water flow and transport utilizes estimates of the statistics of the input parameters to estimate the statistics of the dynamic variables of interest. One of the most studied input parameters, from a stochastic point of view, is the saturated hydraulic conductivity. The statistics of the saturated hydraulic conductivities obtained using core samples and in situ experiments are summarized in Tables 1 and 2. These statistics include the mean, median, standard deviation, skewness, and kurtosis. The usual adjustment for kurtosis is used so that kurtosis of a normal distribution is zero. This adjusted kurtosis is sometimes called the coefficient of excess.

M. Goodrich (manuscript in preparation, Sandia National Laboratories, Albuquerque, New Mexico) utilized the Mann-Whitney test on the saturated conductivities (on *Ksat* but not ln (*Ksat*)) to evaluate whether the means of the various layers are statistically different. This is a nonparametric method that tests whether the means of two independent, random sets of data are different at a specified confidence level. The dispersion (variance) of the sample populations was not considered. Goodrich found that at a confidence level of 90%, the laboratory data could be grouped into three layers composed of the original layers 1, layers 2–5, and layers 6–9. Goodrich also found that the field conductivities can be grouped into three layers which are composed of the original layers 1, layers 2–6, and layers 7–9.

Jacobson [1990] has used directional semivariograms to estimate variance, correlation lengths, and the principal directions for the in situ ln (*Ksat*) for the Las Cruces site. Initially, all the in situ ln (*Ksat*) data from the site were grouped and assumed to have a constant mean and variance. The resulting analysis indicated that the horizontal and vertical correlation lengths were 2.5 and 0.5 m, respectively. Closer inspection of the results indicated that most of the horizontal correlation was due to layers 3–6 and that the remaining layers were essentially uncorrelated. In a more detailed analysis, the data were combined into three groups composed of layers 1 and 2, layers 3–6, and layers 7–9 and analyzed for horizontal correlation length. The semivariograms for the first and last groups showed no horizontal correlation while the group comprising layers 3–6 showed a correlation length of 2.0 m. A vertical sample semivariogram using the data obtained from the three vertical transects showed a correlation length of 0.15 which was considerably lower than the 0.5 m value obtained when all the data were combined into one group.

Equivalent uniform soil and layered soil relationships for the soil water retention curves and the saturated hydraulic conductivity were estimated using the procedures discussed earlier. The parameter values for the resulting models are listed in Table 3 for a uniform soil and layered soil model. Also listed are the mean square errors (MSE) for the water retention models defined as

$$\mathrm{MSE} = \frac{\sum_{i=1}^{N} (\theta(h_i) - \hat{\theta}(h_i))^2}{N - 4} \tag{8}$$

where $\theta(h_i)$ and $\hat{\theta}(h_i)$ are the measured and predicted volumetric water contents for tension h_i. The mean square errors give a measure of "goodness of fit" of each model. This estimate of $\sigma_{\hat{\theta}}^2$ includes the error from the model lack of fit

TABLE 1. Statistics of the Saturated Hydraulic Conductivities

Statistic	$Ksat_{lab}$	ln ($Ksat_{lab}$)	$Ksat_{field}$	ln ($Ksat_{field}$)
Minimum	1.4	0.336	9.3	2.23
Maximum	6,730.6	8.814	12,998	9.473
Points	446	446	445	445
Mean	533.22	5.5988	850.76	6.0236
Median	389.0	5.9635	403.5	6.000
Standard deviation	647.13	1.3207	1421.0	1.2096
Skewness	4.0706	−0.47718	4.9243	−0.075228
Kurtosis	28.114	−0.41594	31.523	0.31451

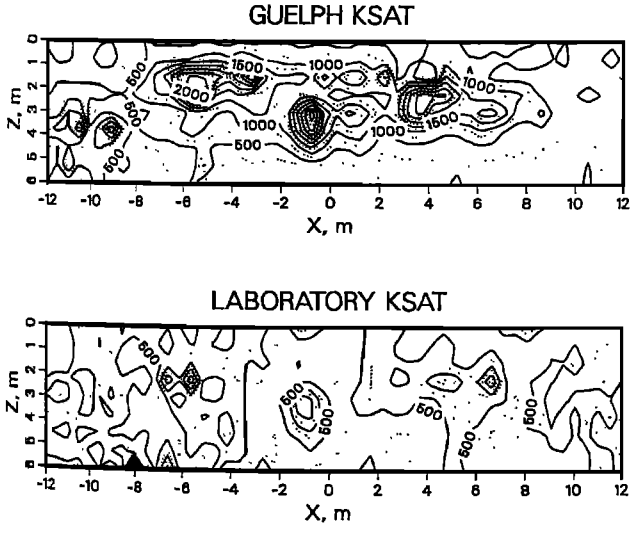

Fig. 4. Comparison between laboratory-based and Guelph permeameter–based saturated hydraulic conductivity; contour spacing between solid lines is 500 cm/d.

TABLE 2. Statistics of the Saturated Hydraulic Conductivities by Layer

Statistic	$Ksat_{lab}$	ln ($Ksat_{lab}$)	$Ksat_{field}$	ln ($Ksat_{field}$)
		Layer 1		
Minimum	226.5	5.423	146.9	4.990
Maximum	1,378.2	7.229	655.7	6.486
Points	50	50	50	50
Mean	592.08	6.2901	375.15	5.869
Median	517.85	6.2495	357.90	5.8800
Standard deviation	270.23	0.43371	124.69	0.35479
Skewness	1.1147	0.16584	0.26123	−0.43545
Kurtosis	0.86950	−0.49580	−0.63059	−0.39801
		Layer 2		
Minimum	39.3	3.671	73.9	4.303
Maximum	1,484.3	7.303	1,478.4	7.299
Points	50	50	50	50
Mean	379.78	5.5212	670.24	6.3889
Median	229.45	5.4355	620.75	6.431
Standard deviation	351.73	0.95130	302.91	0.53592
Skewness	1.2943	0.021465	0.47742	−1.17703
Kurtosis	0.81769	−0.90417	−0.27788	2.8842
		Layer 3		
Minimum	31.4	3.447	65.2	4.177
Maximum	1,186.4	7.079	5,060.3	8.529
Points	48	48	50	50
Mean	416.35	5.5869	1,214.4	6.3684
Median	329.7	5.795	608.15	6.4095
Standard deviation	347.12	1.0507	1,344.7	1.3266
Skewness	0.78597	−0.35225	1.2681	−0.018136
Kurtosis	−0.49456	−1.0838	0.64684	−1.3591
		Layer 4		
Minimum	14	2.639	14	2.639
Maximum	5,103.3	8.538	5,297.5	8.575
Points	49	49	45	45
Mean	690.99	5.7032	1,236.8	6.5415
Median	431.0	6.066	940.4	6.846
Standard deviation	963.96	1.4373	1,315.2	1.2340
Skewness	2.6702	−0.28653	1.7955	−0.73060
Kurtosis	7.9872	−0.63057	2.6555	0.75369
		Layer 5		
Minimum	19.5	2.970	87.9	4.476
Maximum	1,371.8	7.224	10,818.9	9.2890
Points	50	50	50	50
Mean	454.98	5.5212	1,257.8	6.6460
Median	361.05	5.8870	716.05	6.5705
Standard deviation	398.30	1.2822	1,690.22	0.96621
Skewness	0.58290	−0.46608	3.9623	0.24743
Kurtosis	−0.94534	−1.1090	18.891	0.012135
		Layer 6		
Minimum	1.4	0.336	37.4	3.622
Maximum	6,730.6	8.8140	12,998.5	9.4730
Points	49	49	50	50
Mean	790.37	5.8111	2,062.7	6.8030
Median	629.20	6.4440	1,257.1	7.1360
Standard deviation	1,057.7	1.6702	2,917.3	1.4446
Skewness	3.8165	−1.0586	2.5650	−0.40434
Kurtosis	18.546	1.0027	6.0273	−0.34287
		Layer 7		
Minimum	18.8	2.934	65.9	4.188
Maximum	3,166	8.060	1,991.3	7.597
Points	50	50	50	50
Mean	552.15	5.3962	313.57	5.3922
Median	165.7	5.1035	203.80	5.3170
Standard deviation	639.91	1.5192	341.94	0.79358
Skewness	1.5494	0.039101	2.9777	0.66763
Kurtosis	3.4496	−1.5857	10.512	−0.090927
		Layer 8		
Minimum	13.7	2.617	16.9	2.827
Maximum	1,773.0	7.48	1,577.2	7.363
Points	50	50	50	50
Mean	432.17	5.1447	287.33	5.2272
Median	113.05	4.7255	199.35	5.2950
Standard deviation	453.29	1.5686	317.41	0.95720
Skewness	0.73876	−0.057410	2.6876	−0.14497
Kurtosis	−0.41718	−1.6356	7.7594	0.16643
		Layer 9		
Minimum	18.5	2.918	9.3	2.23
Maximum	4,756.6	8.467	1,260.4	7.139
Points	50	50	50	50
Mean	493.78	5.4200	277.32	5.0277
Median	203.3	5.3015	156.3	5.0515
Standard deviation	748.66	1.2957	291.54	1.2415
Skewness	3.9258	0.15322	1.7076	−0.51033
Kurtosis	19.229	−1.0159	2.6122	−0.36468

and the random error. While MSE is not an unbiased estimator of σ_θ^2, the bias will be small when the sample size is large and the errors are independent, additive, and approximately $N(0, \sigma^2)$.

Water Movement During Infiltration

The advance of the wetting front, as visually observed on the trench face, is shown in Figure 5. The data in this figure show a fairly symmetrical, nearly semicircular infiltration front after 34 days of water application. The wetting front has a rather irregular shape on day 14. We suspect that this irregularity was due to excess runoff water which entered the plot accidentally through a failure in the pond liner during a heavy rainstorm.

On day 50 the wetting front had reached the 5.3 m depth. At that time the wetting front had spread about 1 m to the right of the irrigated area and about 0.75 m to the left of the irrigated area. The greater spreading of the wetting front to the right may be due to the infiltration of rainfall on the right side of the irrigated area rather than due to some anisotropy of the formation.

The advance of the wetting front was also determined from the changes in tension in a plane at 0.5 m from and parallel to the trench face. Water tensions were initially very high, but decreased fairly rapidly along the vertical centerline of the irrigated area when the wetting front reached a tensiometer. The tension decreased more slowly at locations not directly under the irrigated area. The time of arrival of the wetting front was taken as the time at which the tension dropped and remained below 100 cm. Note that the results given in Figure 6 show the same trend as in Figure 5. The wetting front appears to progress faster on the right side of the plot where some rainfall most likely entered the plot area. An important difference between Figures 5 and 6 is that the wetting front, as measured with tensiometers, is generally ahead of the wetting front recorded visually on the

TABLE 3. Van Genuchten Parameters for the Las Cruces Test Site: Uniform and Layered Soil Models

Layers	Depth, cm	θ_s	θ_r	α, cm^{-1}	n	K_s, cm/d	MSE × 10^3
			Uniform Soil Model				
all	0–600	0.3209	0.0828	0.05501	1.5093	270.1	1.512
			Layered Soil Model				
1	0–15	0.3483	0.0949	0.04194	1.9026	539.2	0.358
2	15–140	0.3434	0.0914	0.06237	1.5278	250.0	1.007
3	140–205	0.3359	0.0849	0.05960	1.5742	266.9	1.497
4	205–250	0.3129	0.0714	0.06772	1.5373	299.8	1.610
5	250–305	0.3021	0.0716	0.04039	1.5496	250.0	0.688
6	305–370	0.2942	0.0896	0.07029	1.7117	334.0	2.350
7	370–460	0.3104	0.0726	0.02719	1.4177	220.6	0.674
8	460–540	0.3248	0.0834	0.04110	1.3826	171.5	0.646
9	540–600	0.3061	0.0778	0.04679	1.4315	225.9	1.300

trench face. For example, on day 29 the wetting front had reached a depth of about 3.25 m as observed on the trench face but had reached a depth of 3.75 m as measured with tensiometers. One explanation for the slower apparent advance on the trench face is that the initial water content of the soil near the trench face was lower than at 0.5 m inside the trench wall. This is most likely due to water loss caused by evaporation from the exposed trench wall during construction. A lower initial water content requires more water to fill the pore space to a given final water content (near field capacity). Because the applied water flux is the same over the entire irrigated area, a lower initial water content near the trench face would lead to a slower advance of the wetting front.

The advance of the wetting front may also be determined from water content measurements obtained with the neutron probe. The arrival time of the wetting front was taken as the time for which the measured water content increased to a value halfway between the eventual maximum value at a location and the corresponding initial value. While this choice is somewhat arbitrary, the choice will have little effect on the results since the wetting front is very steep. Figures 7 and 8 show the resulting wetting front motion in planes parallel to and perpendicular to the trench face, respectively. Figure 8 clearly shows the slower advance of the wetting front near the trench face as compared to 4 m from the face. The wetting front advance was also somewhat delayed near the end of the irrigated section of the plot (x = 8 m). We suspect that this may be due to horizontal spreading of the water.

One-Dimensional Infiltration Model Results

As discussed earlier, the initial field tensions used for the numerical simulation were obtained from soil samples using a Decagon thermocouple psychrometer (Decagon Devices, Inc., Pullman, Washington). Seven samples were taken from each of nine depths. The seven tensions from each depth were averaged. The resulting average tensions are shown in Table 4. For simulation purposes, an initial tension of 6910 cm H_2O was used for depths less than 60 cm. Linear interpolation was used to estimate the initial tensions at intermediate depths.

A grid spacing of Δz = 2 cm and a time step size of Δt = 0.05 days were used for the finite difference simulation. Reducing the grid and time step size further did not significantly alter the results.

Due to the one-dimensional nature of the numerical model, the best agreement between model prediction and observation should occur along the centerline of the irrigated area where the assumption of one-dimensional flow is most appropriate. We thus restrict our experimental observations to those taken by the neutron probe in access tubes 250, 350, and 450 (see Figure 1). Shown in Figures 9, 10 and 11 are the

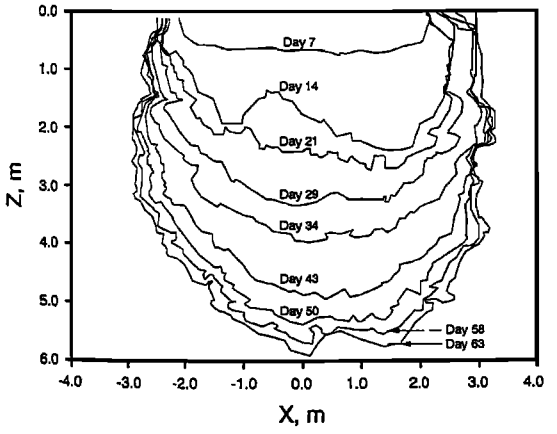

Fig. 5. Advance of the wetting front as visually observed on the trench face.

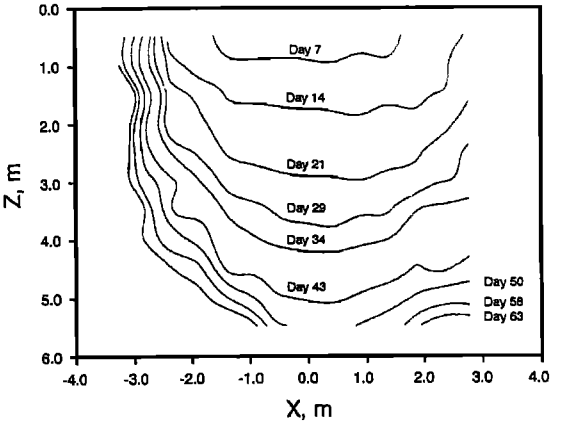

Fig. 6. Advance of the wetting front as determined from the tensiometer measurements.

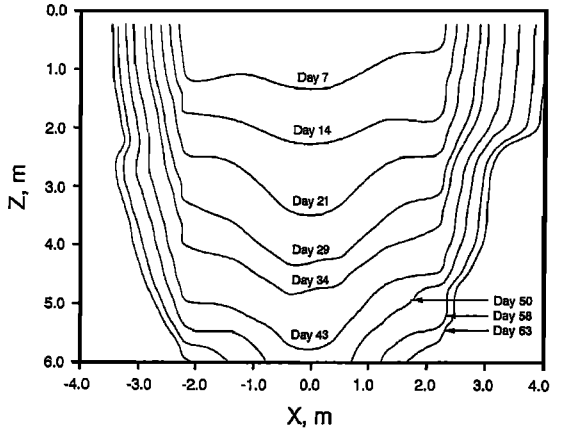

Fig. 7. Advance of the wetting front as determined from the neutron probe measurements: measured in a plane parallel and 4 m from the trench wall.

neutron probe water contents taken from the access tubes on days −2, 19, and 35, respectively. Also shown are the model initial conditions (Figure 9) and the model predictions (Figures 10 and 11) for both the uniform and the layered soil infiltration models. Note that there are discrepancies between the initial water contents as determined from the neutron probe measurements (i.e., those taken on day −2) and the initial water contents as determined from soil property models using the observed initial tensions. These differences are due, in part, to the inability of the uniform or layered soil property models to properly account for local spatial variability in the field conditions. In addition, the θ_r estimated from the laboratory data at 15 bars are often higher than the initial water contents observed in the field. The figures also show that the differences between the layered model predictions and the uniform model predictions are generally smaller than the differences between either model prediction and the observations. Based on visual observation, it would be difficult to claim that the more detailed layered infiltration model produces better results overall than the more simplistic uniform model. Note also that the predictions of the uniform soil model were better at some depths than the layered soil model. This is not surprising

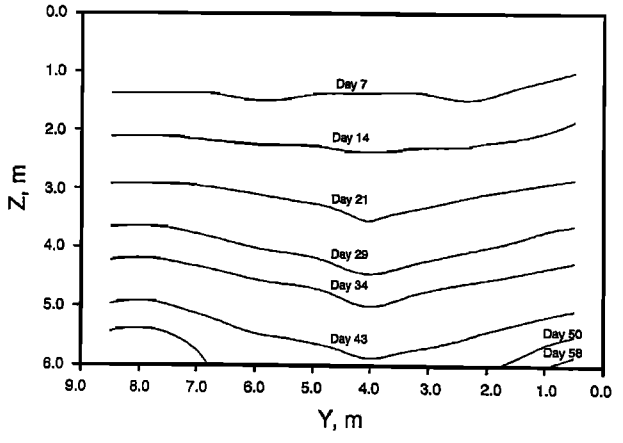

Fig. 8. Advance of the wetting front as determined from the neutron probe measurements: measured in a plane perpendicular to the trench wall.

TABLE 4. Initial Tensions as a Function of Depth

Depth, cm	h, cm H_2O
60	6,910
135	21,530
210	28,860
285	36,980
360	47,090
435	48,020
510	53,300
585	56,330
660	64,940

since the layered soil parameters are effective parameters for the entire layer. The effective soil parameters do not necessarily represent the soil conditions at all point locations within a layer due to the significant spatial variability in the soil hydraulic properties within a layer.

Shown in Table 5 are the correlation coefficients between the experimental and the numerical water contents. The correlation coefficients were evaluated from

$$r = \frac{\sum (x_i - \bar{x})(y_i - \bar{y})}{\left[\sum (x_i - \bar{x})^2 \sum (y_i - \bar{y})^2\right]^{1/2}} \quad (9)$$

Linear interpolation was used to project the numerical results from the finite difference grid to the actual measurement depths. As the results shown in Table 5 indicate, the layered soil model has higher correlation coefficients for day −2 and the uniform soil infiltration model has higher correlation coefficients for day 19. The results are mixed for day 35. While the initial conditions are better modeled using the layered soil model, there is no clear advantage of the layered model over the uniform soil model in predicting infiltration on days 19 and 35.

Shown in Figure 12 is the wetting front location as a function of time as determined from the centerline ($x = 0$) of

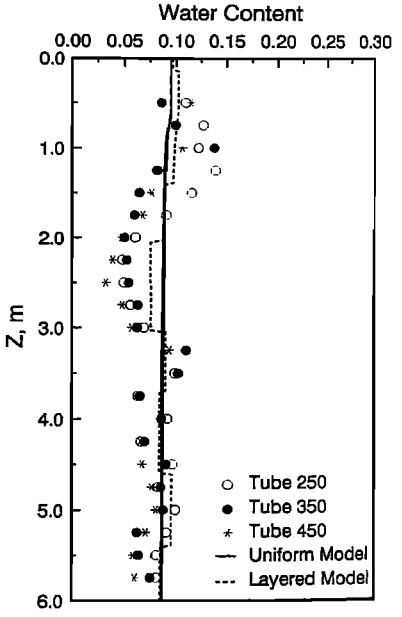

Fig. 9. Observed initial water contents and model initial conditions.

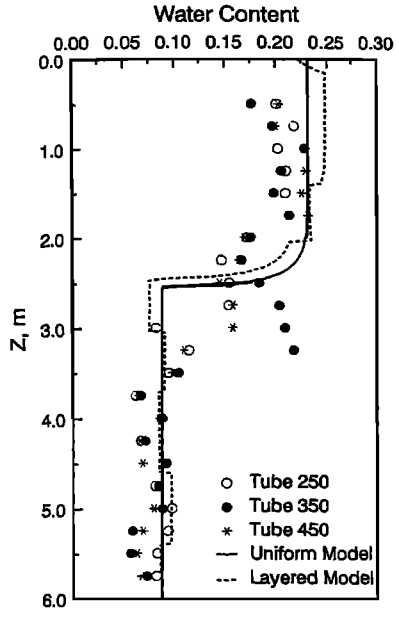

Fig. 10. Water content measurements and model predictions for day 19.

the visual observations, tensiometer readings made 0.25 m on either side of the centerline, and the neutron probe readings from the three centerline neutron probe access tubes, and for the uniform soil numerical model. The wetting front location for the finite difference model was taken to be that location at which the water content has reached a value halfway between the initial water content and the value of water content for which the unsaturated hydraulic conductivity model gives a flux equal to that applied (i.e., 1.82 cm/d) on the surface. The latter value for water content represents the maximum value obtainable during the numerical simulation and is equal to 0.232 cm^3/cm^3 for the hydraulic conductivity model used here.

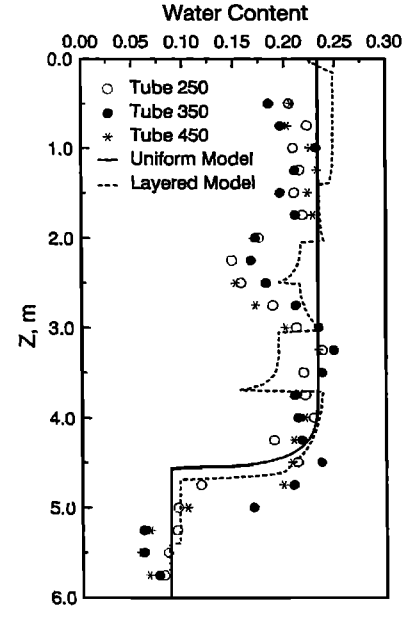

Fig. 11. Water content measurements and model predictions for day 35.

TABLE 5. Correlation Coefficients Between Measured and Predicted Water Contents

Tube Number	Day	Uniform Soil Model	Layered Soil Model
250	−2	0.481	0.795
350	−2	0.277	0.580
450	−2	0.513	0.812
250	19	0.924	0.889
350	19	0.679	0.607
450	19	0.892	0.855
250	35	0.881	0.889
350	35	0.704	0.694
450	35	0.785	0.793

As the results of Figure 12 illustrate, the motion of the wetting front for each of the three neutron probe access tube locations tends to be similar through day 13. From day 14 to day 17, the front velocities appear different, suggesting that the soil has significant lateral spatial variability in the 2.5–3 m depth range. Note that this depth range corresponds to layer 5 of the layered soil property model (see Table 3). These tubes are spaced approximately 2 m apart (see Figure 1). For days 17 and greater, the trends in the front location versus time data tend to be parallel, indicating that the front velocities at greater depths are similar for all three access tube locations.

The results of Figure 12 also show that the wetting front location as predicted by the model lags behind the wetting front location as measured by the neutron probes. In contrast, the predicted wetting front tends to be ahead of those observed visually and inferred from the tensiometers. The simple one-dimensional uniform model predictions are thus bounded by experimental observations. There is surprisingly good agreement between the model predictions and the field observations when one considers that (1) a uniform soil model for the water retention characteristics and saturated hydraulic conductivity were determined from soil samples taken from the opposite side (the north side) of the trench, (2) the water retention characteristics were determined for the drying branch of the hysteresis loop rather than the wetting branch, (3) equation (3) was used for the unsaturated hydraulic conductivity rather than experimental data, (4) the saturated hydraulic conductivity is highly variable over the trench site, and (5) the water contents were estimated from

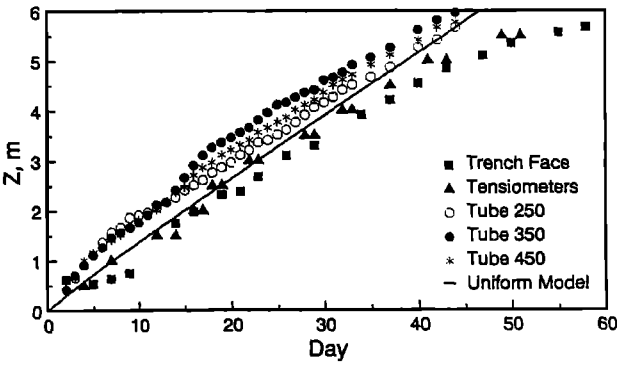

Fig. 12. Comparison of measured and predicted wetting front motion along the centerline ($x = 0$).

the uniform soil retention model and from tensions observed in samples taken from the north side of the trench.

CONCLUSIONS

The saturated hydraulic conductivities show significant variability along the trench wall. Comparisons between the saturated hydraulic conductivity field estimated in situ by the Guelph permeameter method and estimated in the laboratory show a qualitative but not a quantitative agreement. The saturated hydraulic conductivities determined in situ show a larger range of values than do the laboratory-determined conductivities.

Despite the significant spatial variability in the saturated hydraulic conductivity, the movement of the wetting front in the dry unsaturated semiarid soils appears to be fairly homogeneous. Visual observation of the trench face indicates that the wetting front was nearly semicircular after 34 days of water application on the 4-m-wide strip. There were no signs of preferential flow, or water flow through root channels and cracks, and no clearly visible effects on water movement of the soil layering. The tensiometer measurements taken 0.5 m from the trench face and the water content measurements taken on a three-dimensional grid also support the hypothesis that the wetting front motion was fairly uniform.

Comparisons between the predictions of simple one-dimensional infiltration models and observations at two locations show significant differences in the point values of water content due to spatial variability. However, despite these differences, the overall motion of the wetting front was well predicted by the one-dimensional models. This illustrates that predicting the average behavior of water flow is sometimes possible using a simple deterministic model, even though the soil possesses significant spatial variability in the saturated hydraulic conductivity. The use of a layered soil property model rather than the simpler uniform soil property model did not appear to improve the prediction of infiltration. This suggests that increasing the spatial resolution of the deterministic characterization of the site in the vertical direction does not always improve the model predictions. Uncertainties due to horizontal spatial variability and due to other difficulties associated with experimental characterization appear to be more significant. The effect of layering may be more significant for higher water application rates such as occurs during surface ponding.

Acknowledgments. The authors wish to acknowledge the support from the U.S. Nuclear Regulatory Commission and the U.S. Environmental Protection Agency. The advice of Lynn Gelhar and Dennis McLaughlin from the Massachusetts Institute of Technology, Glendon Gee from Battelle Pacific Northwest Laboratories, and Tom Nicholson from the U.S. Nuclear Regulatory Commission with the design and execution of the experiment is gratefully acknowledged. Finally, this project could not have been done without the help of Warren Strong, Joe Vinson, Jim Bilskie, Hesham Elabd, Mohammed Nash, Allan Schneeberger, Indrek Porro and Alex Toorman.

REFERENCES

Biggar, J. W., and D. R. Nielsen, Spatial variability of leaching characteristics of a field soil water, *Water Resour. Res., 12*, 78–84, 1976.

Computer Associates, CA–DISSPLA, version 11, Garden City, N. Y., 1988.

Dagan, C., and E. Bresler, Solute transport in unsaturated heterogeneous soil at field scale, 1, Theory, *Soil Sci. Soc. Am. J., 43*, 461–467, 1979.

Elrick, D. E., R. W. Sheard, and N. Baumgartner, A simple procedure for determining the hydraulic conductivity and water retention of putting green soil mixtures, paper presented at the Fourth International Turfgrass Research Conference, Int. Turfgrass Soc., Guelph, Ont., Canada, July 19–23, 1980.

Gelhar, L. J., and C. L. Axness, Three-dimensional stochastic analysis of macrodispersion in aquifiers, *Water Resour. Res., 19*(1), 161–180, 1983.

Hills, R. G., I. Porro, D. B. Hudson, and P. J. Wierenga, Modeling one-dimensional infiltration into very dry soils, 1, Model development and evaluation, *Water Resour. Res., 25*(6), 1259–1269, 1989*a*.

Hills, R. G., D. B. Hudson, I. Porro, and P. J. Wierenga, Modeling one-dimensional infiltration into very dry soils, 2, Estimation of the soil water parameters and model predictions, *Water Resour. Res., 25*(6), 1271–1282, 1989*b*.

Hills, R. G., D. B. Hudson, and P. J. Wierenga, Spatial variability at the Las Cruces Trench Site, Proceedings of the Workshop on Indirect Methods for Estimating the Hydraulic Properties of Unsaturated Soils, report, U.S. Salinity Lab. and Dep. of Soil and Environ. Sci., Univ. of Calif., Riverside, in press, 1991.

Jacobson, E. A., Estimation of two-dimensional covariance function from directional semi-variograms for field measured saturated hydraulic conductivities, paper presented at International Conference on Validation of Flow and Transport Models for the Unsaturated Zone, Dep. of Agron. and Hort., N. M. State Univ., Ruidoso, N. M., May 23–26, 1988.

Jacobson, E. A., Investigation of the spatial correlation of saturated hydraulic conductivities from a vertical wall of a trench, paper presented at the Canadian/American Conference on Hydrogeology—Parameter Identification and Estimation for Aquifer and Reservoir Characterization, Alta. Res. Counc., Assoc. of Groundwater Sci. and Eng., Calgary, Alta., Canada, Sept. 18–20, 1990.

Montaglou, A., and L. W. Gelhar, Large scale models of transient unsaturated flow and contaminant transport using stochastic methods, *Tech. Rep. 299*, Ralph H. Parsons Lab., Dep. of Civ. Eng., Mass. Inst. of Technol., Cambridge, Mass., 1985.

Mualem, Y., A new model for predicting the hydraulic conductivity of unsaturated porous media, *Water Resour. Res., 12*, 513–522, 1976.

Peck, A. J., Field variability of soil physical properties, *Adv. Irrig., 2*, 189–221, 1983.

Reynolds, W. D., and D. E. Elrick, In situ measurement of field-saturated hydraulic conductivity, sorptivity, and the alpha parameter using the Guelph permeameter, *Soil Sci., 140*, 292–302, 1985.

Russo, D., and E. Bresler, Soil hydraulic properties as stochastic properties, 1, Analysis of field spatial variability, *Soil Sci. Soc Am. J., 45*, 682–687, 1981.

SAS Institute, SAS users guide: Statistics, version 5, Cary, N. C., 1985.

van Genuchten, M. T., Calculating the unsaturated hydraulic conductivity with a new closed-form analytical model, *Rep. 78-WR-08*, 63 pp., Dep. of Civ. Eng., Princeton Univ., Princeton, N. J., 1980.

Warrick, A. W., and D. R. Nielsen, Spatial variability of soil physical properties in the field, in *Applications of Soil Physics*, edited by D. Hillel, pp. 319–344, Academic, San Diego, Calif., 1980.

Webster, R., and H. E. de la Cuanalo, Soil transect correlograms of North Oxfordshire and their interpretation, *J. Soil Sci., 26*, 176–194, 1975.

Wierenga, P. J., J. M. H. Hendrickx, M. H. Nash, J. Ludwig, and L. A. Daugherty, Variation of soil and vegetation with distance along a transect in the Chihuahuan Desert, *J. Arid Environ., 13*, 53–63, 1987.

Wierenga, P. J., D. Bachelet, J. R. Bilskie, H. Elabd, D. B. Hudson, M. Nash, I. Porro, W. R. Strong, A. Toorman, and J. Vinson, Validation of stochastic flow and transport models for unsaturated

soils, *Res. Rep. 88-SS-03*, Dep. of Agron. and Hort., N. M. State Univ., Las Cruces, 1988.

Wierenga, P. J., A. F. Toorman, D. B. Hudson, J. Vinson, M. Nash, and R. G. Hills, Soil physical properties at the Las Cruces trench site, *Rep. NUREG/CR-5441*, U.S. Nucl. Regul. Comm., Washington, D. C., 1989.

Yeh, T.-C. J., L. W. Gelhar, and A. L. Gutjahr, Stochastic analysis of unsaturated flow in heterogeneous soils, 1, Statistically isotropic media, *Water Resour. Res.*, *21*(4), 447–456, 1985*a*.

Yeh, T.-C. J., L. W. Gelhar, and A. L. Gutjahr, Stochastic analysis of unsaturated flow in heterogeneous soils, 2, Statistical anisotropic media with variable α, *Water Resour. Res.*, *21*(4), 457–464, 1985*b*.

Yeh, T.-C. J., L. W. Gelhar, and A. L. Gutjahr, Stochastic analysis of unsaturated flow in heterogeneous soils, 3, Observations and applications, *Water Resour. Res.*, *21*(4), 465–471, 1985*c*.

R. G. Hills, Mechanical Engineering Department, New Mexico State University, Las Cruces, NM 88003.

D. B. Hudson and P. J. Wierenga, Department of Soil and Water Science, University of Arizona, Tucson, AZ 85721.

(Received November 20, 1989;
revised May 22, 1991;
accepted June 10, 1991.)